Since January 2020 Elsevier has created a COVID-19 resource centre with free information in English and Mandarin on the novel coronavirus COVID-19. The COVID-19 resource centre is hosted on Elsevier Connect, the company's public news and information website.

Cell Reports

Activation of the SARS-CoV-2 Receptor *Ace2* through JAK/STAT-Dependent Enhancers during Pregnancy

Graphical Abstract

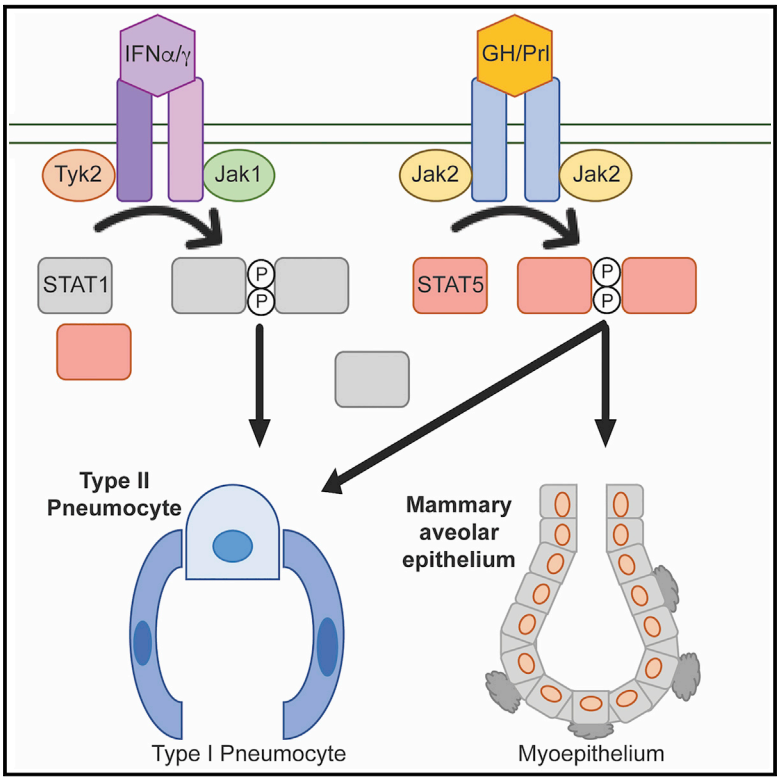

Authors

Lothar Hennighausen, Hye Kyung Lee

Correspondence

lotharh@nih.gov (L.H.),
hyekyung.lee@nih.gov (H.K.L.)

In Brief

Hennighausen and Lee find that increased expression of the SARS-CoV-2 receptor *Ace2* in mammary tissue of mice during pregnancy and lactation is controlled through the hormone-activated JAK/STAT5 signaling pathway. Their findings suggest the possibility of vertical transmission of SARS-CoV-2 through breast milk and non-pulmonary tissue damage.

Highlights

- *Ace2* expression is induced in the mammary glands of pregnant and lactating mice
- Gene enhancers are activated by the prolactin-activated transcription factors STAT5A/B
- Deletion of the *Stat5a* gene mitigates enhancer formation and *Ace2* expression
- *Ace2* levels also increase in lung tissue during lactation

Hennighausen & Lee, 2020, Cell Reports *32*, 108199
September 29, 2020
https://doi.org/10.1016/j.celrep.2020.108199

Cell Reports

CellPress
OPEN ACCESS

Report

Activation of the SARS-CoV-2 Receptor *Ace2* through JAK/STAT-Dependent Enhancers during Pregnancy

Lothar Hennighausen[1,2,*] and Hye Kyung Lee[1,*]
[1]Laboratory of Genetics and Physiology, National Institute of Diabetes and Digestive and Kidney Diseases, U.S. National Institutes of Health, Bethesda, MD 20892, USA
[2]Lead Contact
*Correspondence: lotharh@nih.gov (L.H.), hyekyung.lee@nih.gov (H.K.L.)
https://doi.org/10.1016/j.celrep.2020.108199

SUMMARY

ACE2 binds the coronavirus SARS-CoV-2 and facilitates its cellular entry. Interferons activate *ACE2* expression in pneumocytes, suggesting a critical role of cytokines in SARS-CoV-2 target cells. Viral RNA was detected in breast milk in at least seven studies, raising the possibility that *ACE2* is expressed in mammary tissue during lactation. Here, we show that *Ace2* expression in mouse mammary tissue is induced during pregnancy and lactation, which coincides with the activation of intronic enhancers. These enhancers are occupied by the prolactin-activated transcription factor STAT5 and additional regulatory factors, including RNA polymerase II. Deletion of *Stat5a* results in decommissioning of the enhancers and an 83% reduction of *Ace2* mRNA. We also demonstrate that *Ace2* expression increases during lactation in lung, but not in kidney and intestine. JAK/STAT components are present in a range of SARS-CoV-2 target cells, opening the possibility that cytokines contribute to the viral load and extrapulmonary pathophysiology.

INTRODUCTION

Angiotensin-converting enzyme 2 (ACE2), the receptor for SARS-associated coronavirus (SARS-CoV) (Imai et al., 2005) and SARS-CoV-2 (Hoffmann et al., 2020), has been detected in a range of target cells, including absorptive enterocytes (Lamers et al., 2020), colon organoids (Stanifer et al., 2020), small intestine and colonocytes (Lee et al., 2020), secretory goblet cells (Zhao et al., 2020), the olfactory system (Brann et al., 2020) and several epithelial cell types (Brann et al., 2020; Lukassen et al., 2020; Qi et al., 2020). Although SARS-CoV-2 infection of lung epithelium is a critical driver of disease, extrapulmonary manifestations of coronavirus disease 2019 (COVID-19) infection (Gupta et al., 2020) have been associated with direct viral damage of tissues that carry the ACE2 receptor, such as intestinal enterocytes and renal tissue (Monteil et al., 2020). Deciphering the regulation of the *ACE2* gene in SARS-CoV-2 target cells is a step forward in linking ACE2 levels with viral damage and COVID-19 pathology. This is relevant not only in the context of cytokine storms but also in patients with different physiological conditions, such as pregnancy and lactation.

Although a body of work has focused on the pathology of COVID-19 during pregnancy (Khalil et al., 2020), the extent to which hormones control *ACE2* expression during pregnancy and lactation, and possibly the susceptibility of cells to SARS-CoV-2 infection, has not been investigated. One hallmark of pregnancy is the development of functional mammary tissue that produces large quantities of milk during lactation. Both mammary development and milk production are governed by the cytokine prolactin and the downstream Janus kinase (JAK)/signal transducer and activator of transcription (STAT) signaling pathway (Liu et al., 1997). STAT5 is activated by prolactin and is essential for both mammary development and milk production. Its role in the activation of transcriptional enhancers during pregnancy is well established (Lee et al., 2018; Yamaji et al., 2013).

SARS-CoV-2 RNA has been detected in breast milk of infected individuals (Bastug et al., 2020; Buonsenso et al., 2020; Costa et al., 2020; Groß et al., 2020; Kirtsman et al., 2020; Tam et al., 2020; Wu et al., 2020), suggesting the possibility of vertical transmission. However, the presence of ACE2 in mammary tissue and its regulation during pregnancy has not been investigated. Because interferons (IFNs) can activate *ACE2* expression in pneumocytes (Ziegler et al., 2020), the question arose whether other cytokines can regulate *ACE2* in mammary cells through the JAK/STAT pathway. In addition, the widespread expression of JAK/STAT components and associated receptors, their overlapping activities, and potential redundancy might affect *ACE2* expression in a range of epithelial cell types. Based on the presence of SARS-CoV-2 RNA in milk, we investigated the presence and regulation of *Ace2* in mammary tissue throughout pregnancy and lactation in mice. Specifically, we asked whether the hormonal milieu results in the activation of enhancer structures that induce *Ace2* expression and the genetic role of the transcription factor STAT5 during pregnancy and lactation.

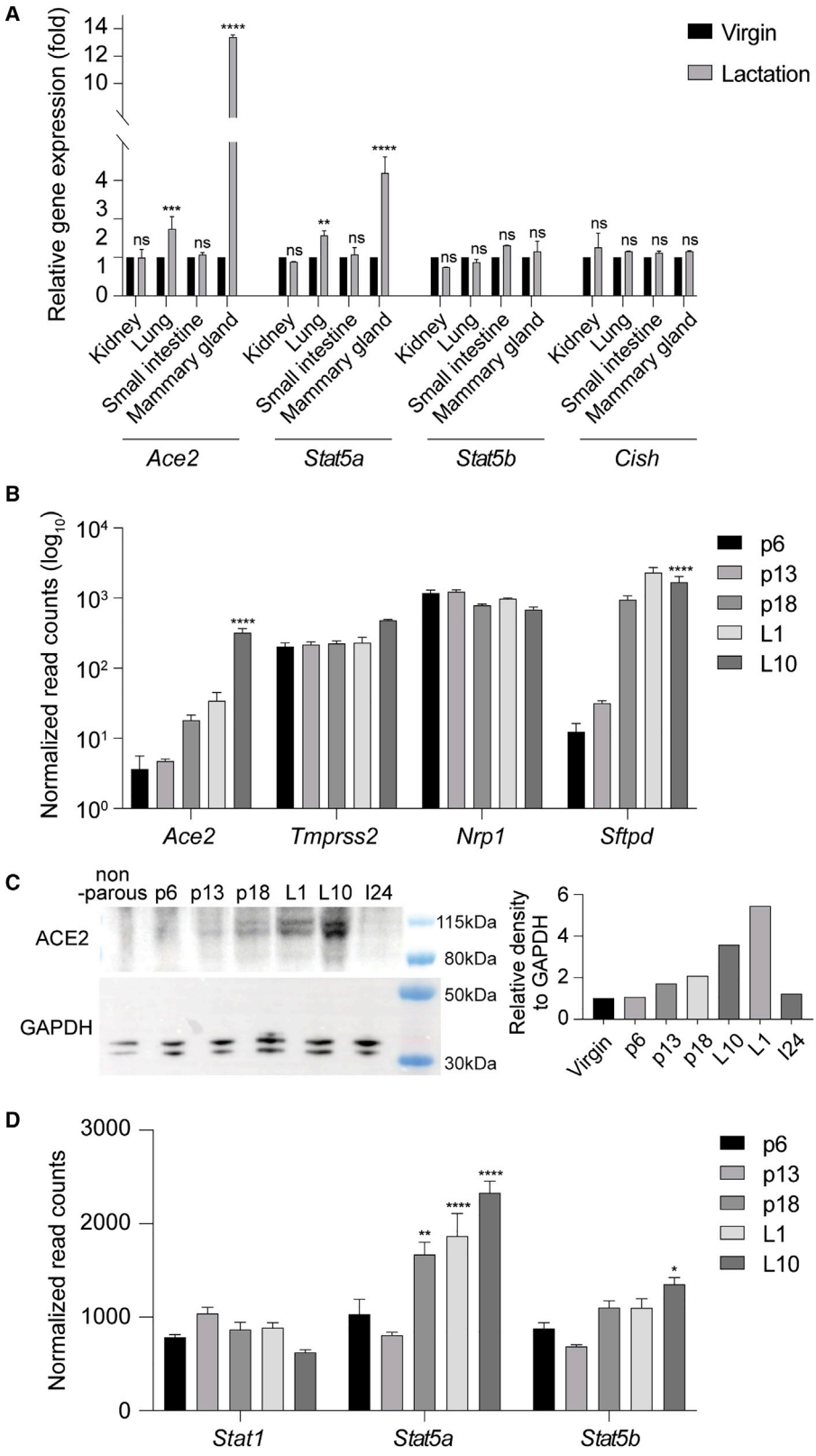

(legend on next page)

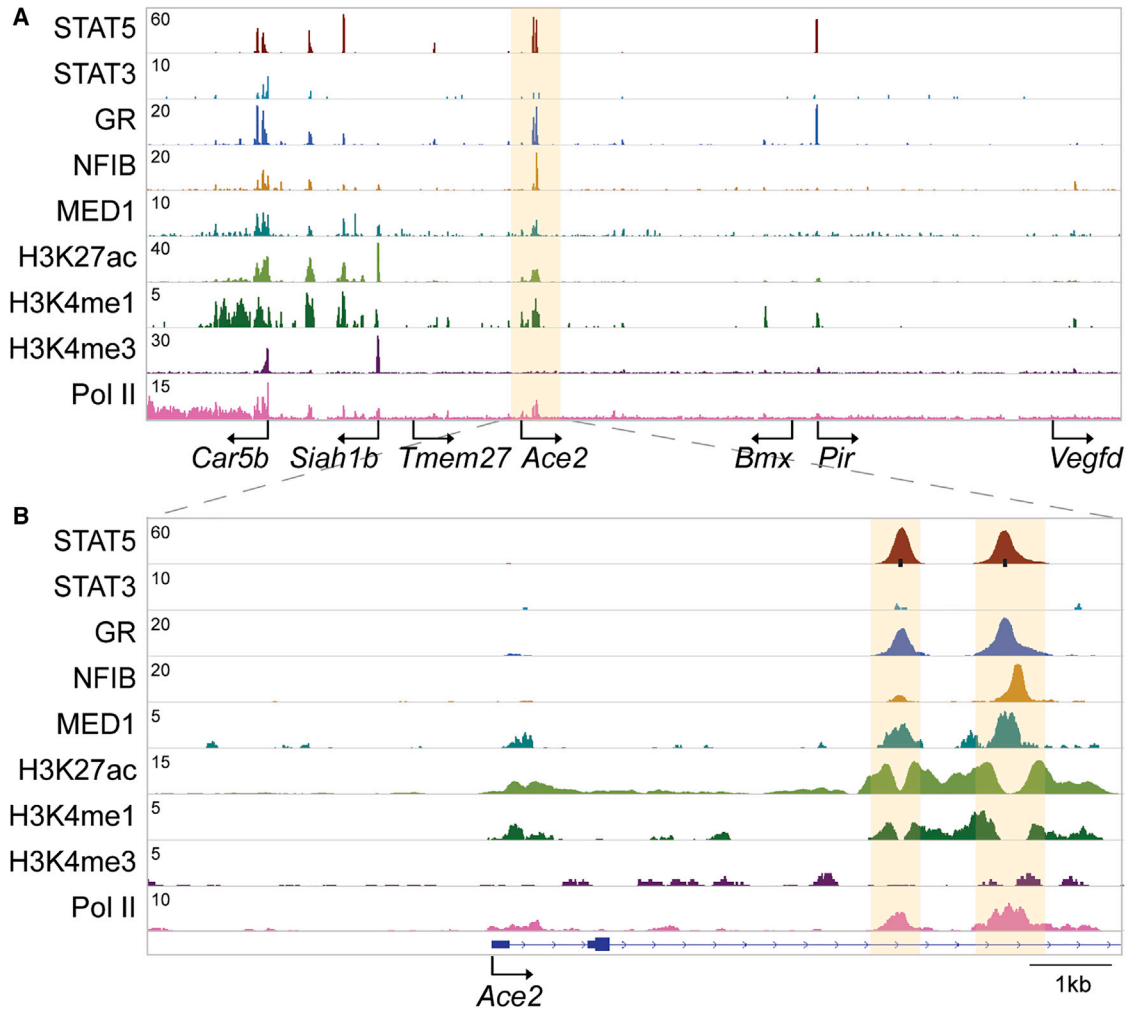

Figure 2. Occupation of a Candidate *Ace2* Enhancer during Lactation

(A and B) ChIP-seq data for STAT5, STAT3, GR, NFIB, MED1, and histone markers H3K27ac and H3K4me3 provided structural information about the locus including the *Ace2* gene in L10 mammary tissue. Solid arrows indicate the orientation of genes. Black bars indicate GAS motifs (STAT binding sites). Orange shades indicate candidate regulatory elements.

RESULTS

Ace2 Expression in Mammary Tissue during Pregnancy

Expression of the *ACE2* gene in type II pneumocytes is activated by IFNs (Ziegler et al., 2020), opening the possibility that the cytokine storm in COVID-19 patients, and peptide hormones in general, might lead to increased levels of ACE2 in a range of putative SARS-CoV-2 target tissues. This in turn could result in elevated viral load and subsequent tissue damage. To explore the possibility that *Ace2* gene expression is regulated by cytokines through the family of STAT transcription factors, we initially mined scRNA-seq data (Ziegler et al., 2020). The abundant presence of interferon receptor (IFNAR) and its downstream mediators JAK1, JAK2, and TYK2, as well as STAT1, STAT3, and STAT5 supports a pivotal contribution of the JAK/STAT pathway in the activation of *ACE2* by IFN-α/β and IFN-γ. STAT1 levels are increased sharply in cells treated with IFNs, supporting the notion that an autoregulatory loop (Yuasa and Hijikata, 2016) is needed to activate IFN target genes.

Figure 1. *Ace2* Activation in Mammary Tissue during Lactation

(A) *Ace2* and *Stat5* mRNA levels in mammary tissue from non-parous and L10 wild-type mice were measured by qRT-PCR and normalized to *Gapdh* levels. The *Cish* gene served as a control. Results are shown as the means ± SEM of independent biological replicates (n = 3). ANOVA was used to evaluate the statistical significance of differences between virgin and lactation mice. ns, not significant. (B and D) mRNA levels of genes in mouse mammary tissue at different stages of pregnancy and lactation were measured by RNA-seq. Day 6 of pregnancy (p6), day 13 of pregnancy (p13), day 18 of pregnancy (p18), L1, and L10. Two-way ANOVA followed by Tukey's multiple comparisons test was used to evaluate the statistical significance of differences in p6 and other developmental stages. *$p < 0.05$, **$p < 0.001$, ****$p < 0.00001$.

(C) ACE2 protein level was analyzed by western blot in mammary tissues of virgin mice, as well as pregnant and lactating mice.

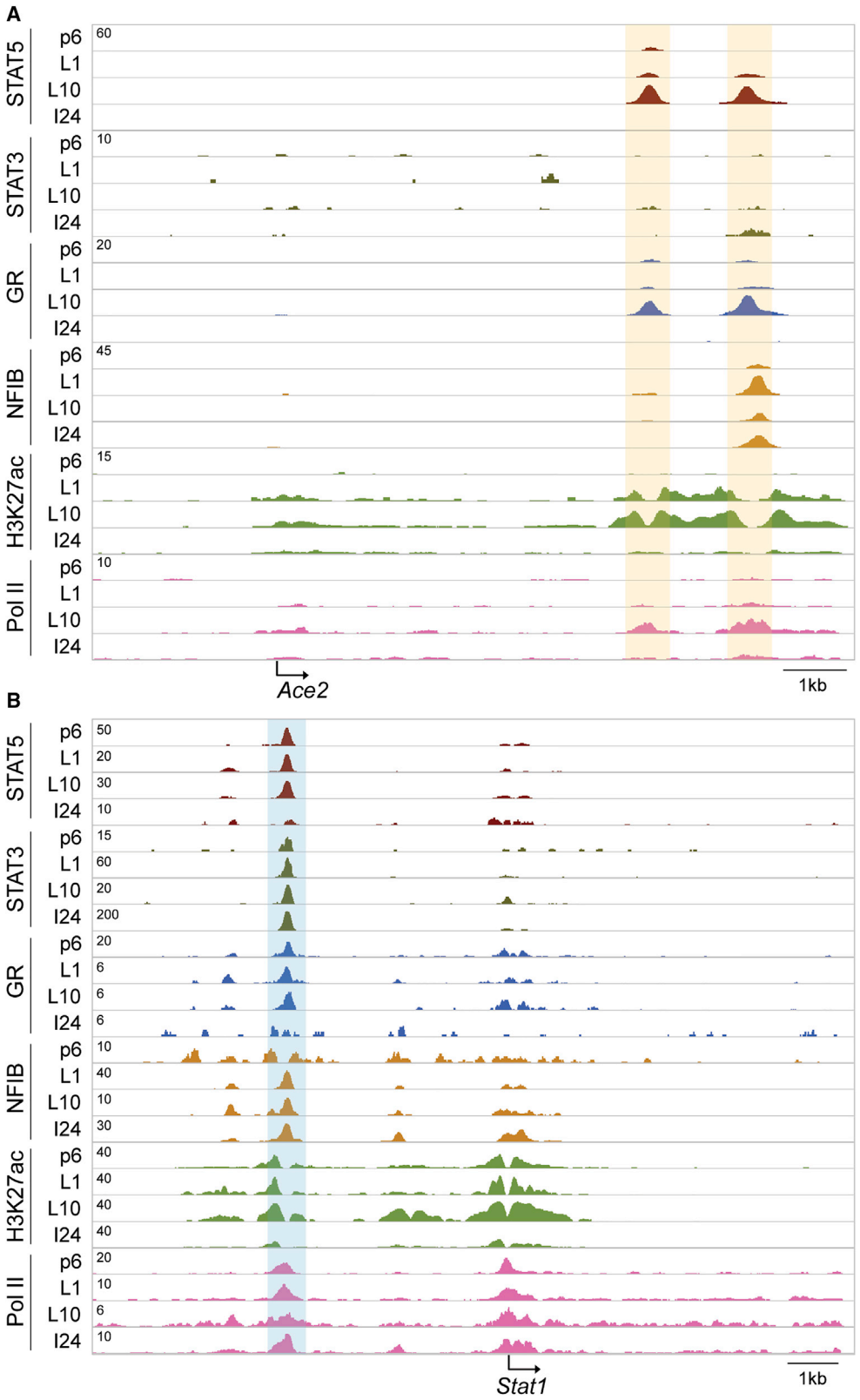

(legend on next page)

The presence of a range of cytokine receptors and JAK/STAT components suggests that *ACE2* might be activated by a selection of cytokines including prolactin, which controls mammary development and other physiological parameters during pregnancy and lactation. In a first step, we determined whether *Ace2* expression in lung, kidney, and intestine, well-established SARS-CoV-2 target tissues, is regulated during pregnancy and lactation in female mice (Figure 1A). Although *Ace2* levels in kidney and intestine were equivalent between non-parous and day 10 of lactation (L10) mice, a 2-fold increase was observed in lung tissue, which harbors the prolactin receptor and all necessary downstream signaling components. Following up on reports of SARS-CoV-2 RNA in milk, we explored *Ace2* expression in mammary tissue. *Ace2* mRNA was present in mammary tissue, and an approximately 13-fold increase was observed during lactation (Figure 1A). Gene expression in mammary tissue during pregnancy and lactation is activated by prolactin through STAT5 (Liu et al., 1997), and increased expression of *Stat5a* during lactation is the result of an autoregulatory enhancer (Metser et al., 2016). Next, we mined RNA sequencing (RNA-seq) data from our lab and demonstrated increased *Ace2* expression throughout pregnancy and lactation (Figure 1B) with a pattern similar to that of other prolactin-regulation genes (Lee et al., 2018; Yamaji et al., 2013). In concordance, ACE2 protein levels increased during pregnancy and lactation (Figure 1C). In contrast, expression of the ACE2-associated serine protease *Tmprss2* and the novel putative SARS-CoV-2 receptor neuropilin-1 (*Nrp1*) was not further induced, suggesting that they are not under overt control of the JAK/STAT pathway. Surfactant protein D (SFTPD) is a secreted protein expressed in both lung tissue and mammary tissue, and its gene is induced during pregnancy and lactation (Figure 1B). Expression of *Stat5a*, a key driver of prolactin signaling in mammary tissue, increases during pregnancy and lactation (Figure 1D).

Activation of STAT5 Enhancers

The *Ace2* expression pattern during pregnancy and lactation mirrored that of mammary-specific prolactin-regulated genes, suggesting a key role of STAT5 in its regulation. To explore this further, we dug deeper and analyzed chromatin immunoprecipitation sequencing (ChIP-seq) profiles aimed at identifying mammary regulatory elements at L10 (Figure 2). ChIP-seq for histone H3 lysine 4 monomethylation (H3K4me1) and histone H3 lysine 27 acetylation (H3K27ac) suggested the presence of several enhancers in the extended locus (Figure 2A), with two putative intronic enhancers in the *Ace2* gene (Figure 2B). STAT5 binding coincided with two GAS motifs, which constitute bona fide STAT binding sites. STAT5 binding was at sequences void of H3K27ac marks, suggesting direct transcription factor binding to histone-free areas. In addition to STAT5, co-occupancy of several other transcription factors, including the glucocorticoid receptor (GR), nuclear factor 1 B (NFIB) and mediator complex subunit 1 (MED1), was observed (Figure 2B). Because of the absence of bona fide binding motifs for these factors, we propose that they bind by contacting STAT5, rather than binding independently to DNA. RNA polymerase II (RNA Pol II) occupancy supports the validity of this regulatory region. No STAT3 occupancy was observed, suggesting a predominance of STAT5.

To directly link the activation of the intronic enhancer to increased *Ace2* expression, we analyzed ChIP-seq datasets throughout pregnancy, lactation, and involution (Figure 3). Although signs of enhancers were detected at day 6 of pregnancy (p6), complete occupation with transcription factors and activation occurred only at L10 (Figure 3A). Upon cessation of lactation, the enhancers were decommissioned within 24 h of involution (I24), similar to what was observed with other pregnancy-regulated genes (Willi et al., 2016). Notably, coinciding with the loss of STAT5 occupancy at the enhancers, limited STAT3 binding was observed, similar to that of other mammary genes (Willi et al., 2016). The *Stat1* enhancer served as a control (Figure 3B).

Ace2 Is under Direct STAT5 Control

Although the ChIP-seq experiments strongly suggest that *Ace2* expression is under the control of STAT5, experimental genetics is required to proof a direct relationship. To directly address the contribution of STAT5, we analyzed mammary tissue from two lines of *Stat5* mutant mice (Yamaji et al., 2013). One line lacked the two *Stat5a* alleles (*Stat5a*$^{-/-}$; *Stat5b*$^{+/+}$), and the other lacked both *Stat5* genes. In lactating mammary tissues, STAT5a accounts for at least 75% of total STAT5 (Yamaji et al., 2013). In the absence of STAT5a, *Ace2* expression at day 1 of lactation (L1) was reduced by 83% (Figure 4A). A similar reduction was observed in the absence of both *Stat5* genes, suggesting an insignificant contribution of STAT5b.

ChIP-seq experiments validated the absence of STAT5a binding in mice lacking both *Stat5a* alleles (Figure 4B). In addition, STAT5b binding was impaired in these mutant mice, suggesting that the presence of STAT5a is required for Stat5b binding or that a specific threshold of STAT5 is needed. The *Cish* gene served as a control for STAT5b binding in mutant mice (Figure 4B).

DISCUSSION

Our study directly demonstrates that the *Ace2* gene is expressed in mammary tissue and activated during pregnancy and lactation through intronic enhancers built on the transcription factor STAT5. Our findings built a framework needed to assess and understand the contributions of a range of cytokines faced under various physiological conditions in extrapulmonary manifestations of COVID-19 (Gupta et al., 2020). The hormonal milieu associated with pregnancy and lactation is unique, and high levels of prolactin, a cytokine that activates the pan-JAK/STAT signaling pathway, control hundreds of target genes. Although these target genes have been well characterized in mammary

Figure 3. Assembly of the *Ace2* Enhancer during Pregnancy and Lactation

(A and B) ChIP-seq data for transcription factors and histone markers provided enhancer structures of the *Ace2* locus in mammary tissues at p6, L1, L10, and I24 after L10. Solid arrows indicate the orientation of genes. Orange and blue shades indicate regulatory elements. The *Stat1* gene served as a ChIP-seq control.

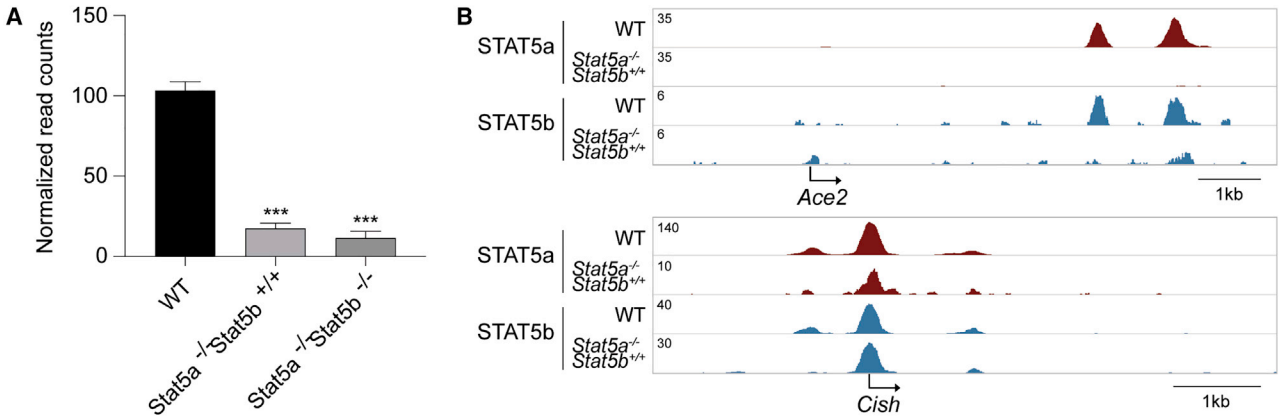

Figure 4. STAT5 Is Required for *Ace2* Expression and Enhancer Activation in Mammary Epithelium

(A) *Ace2* mRNA levels in mouse mammary tissue from wild-type and *Stat5* mutant mice were measured by RNA-seq (Yamaji et al., 2013). One-way ANOVA was used to evaluate the statistical significance of differences in WT and mutants. ***$p < 0.0001$.

(B) STAT5 enhancers were profiled using ChIP-seq data from wild-type and *Stat5* mutant tissue.

tissue (Yamaji et al., 2013), less is known about them in other cell types. Because cytokine receptors and downstream JAK/STAT components are present in a range of cell types, it can be predicted that pregnancy hormones significantly, and possibly cell-preferentially, affect genetic programs. Our finding that *Ace2* expression was increased in lung tissue during lactation is significant, because it might place women during pregnancy and lactation at a higher risk. A retrospective study would be warranted.

Although SARS-CoV-2 has been detected in breast milk in at least seven studies and our research has demonstrated that its receptor ACE2 is present in mammary tissue and highly induced during lactation, the impact of these findings on COVID-19 requires further investigation. Interrogating the mechanism of *Ace2* regulation observed in mammary tissue during pregnancy through the use of cell lines will likely be futile, because cell lines do not mimic the complexity of functional mammary tissue. The use of primary tissue and organoids from pregnant women cannot be pursued. Vertical transmission of SARS-CoV-2 through breast feeding (Lackey et al., 2020) would depend on the infectivity of the virus in milk and upon passing through the gastrointestinal tract. Because human colonic organoids and gut enterocytes can be productively infected *in vitro* (Lamers et al., 2020; Stanifer et al., 2020), the transmission of milk-borne SARS-CoV-2 to the infant needs further examination. Clearly, other viruses are vertically transmitted through milk (Reid et al., 1984).

Based on a pneumocyte study (Ziegler et al., 2020) and our results, we predict that cytokines regulate ACE2 levels in a range of SARS-CoV-2 target cells by drawing on JAKs and STAT transcription factors. Although the impact on virus-induced non-pulmonary pathology remains to be determined, the effectiveness of JAK/STAT pathway inhibitors in mitigating ACE2 levels needs to be evaluated. Interfering with individual STATs results in compensational recruitment of other STAT members to cytokine receptors (Cui et al., 2007), with all its transcriptional consequences (Hennighausen and Robinson, 2008). In contrast, JAK inhibitors could prove effective. They are used to suppress cytokine storms induced by the pan-JAK/STAT pathway, and inflammation in COVID-19 patients treated with the JAK1/2 inhibitor ruxolitinib is reduced (La Rosée et al., 2020). Similarly, baricitinib, which inhibits the proinflammatory signal of several cytokines by suppressing JAK1/JAK2, has a beneficial impact in COVID-19 patients (Cantini et al., 2020).

Future investigations aimed at understanding the mechanism of *ACE2* gene regulation in SARS-CoV-2 target tissues, such as kidney and intestine, need to address the range of cytokines and all components of the pan-JAK-STAT pathway. The presence of JAK/STAT components and their respective receptors is likely not sufficient to activate *Ace2* expression, as shown in kidney and intestine of this study, and additional cell-specific transcription factors and receptors might be required. Candidates are mammary-enriched transcription factors NFIB, ELF5, and GR. Based on our study and previous data (Ziegler et al., 2020) it is likely that IFNs and prolactin can activate *Ace2* expression through STAT1 and STAT5. By including steroid hormones and males and females of different ages in future studies, insight into the sex differences seen in COVID-19 morbidity and mortality (Galbadage et al., 2020) might emerge.

STAR★METHODS

Detailed methods are provided in the online version of this paper and include the following:

- KEY RESOURCES TABLE
- RESOURCE AVAILABILITY
  - Lead Contact
  - Materials Availability
  - Data and Code Availability
- EXPERIMENTAL MODEL AND SUBJECT DETAILS
  - Animals
- METHOD DETAILS
  - Chromatin immunoprecipitation sequencing (ChIP-seq) analysis
  - RNA-seq analysis

- Western blot
- RNA isolation and quantitative real-time PCR (qRT–PCR)

- QUANTIFICATION AND STATISTICAL ANALYSIS

ACKNOWLEDGMENTS

This work was supported by the Intramural Research Program (IRP) of the National Institute of Diabetes and Digestive and Kidney Diseases (NIDDK) and used the computational resources of the NIH HPC Biowulf cluster (http://hpc.nih.gov).

AUTHOR CONTRIBUTIONS

H.K.L. and L.H. designed the study. H.K.L. performed experiments, data analysis, and computational analysis. H.K.L. and L.H. supervised the study and wrote the manuscript. Both authors approved the manuscript.

DECLARATION OF INTERESTS

The authors declare no competing interests.

Received: May 9, 2020
Revised: July 20, 2020
Accepted: September 3, 2020
Published: September 6, 2020

REFERENCES

Anders, S., Pyl, P.T., and Huber, W. (2015). HTSeq—a Python framework to work with high-throughput sequencing data. Bioinformatics *31*, 166–169.

Bastug, A., Hanifehnezhad, A., Tayman, C., Ozkul, A., Ozbay, O., Kazancioglu, S., and Bodur, H. (2020). Virolactia in an Asymptomatic Mother with COVID-19. Breastfeed Med. *15*, 488–491.

Bolger, A.M., Lohse, M., and Usadel, B. (2014). Trimmomatic: a flexible trimmer for Illumina sequence data. Bioinformatics *30*, 2114–2120.

Brann, D.H., Tsukahara, T., Weinreb, C., Lipovsek, M., Van den Berge, K., Gong, B., Chance, R., Macaulay, I.C., Chou, H.-J., Fletcher, R.B., et al. (2020). Non-neuronal expression of SARS-CoV-2 entry genes in the olfactory system suggests mechanisms underlying COVID-19-associated anosmia. Sci. Adv. *6*, eabc5801.

Buonsenso, D., Costa, S., Sanguinetti, M., Cattani, P., Posteraro, B., Marchetti, S., Carducci, B., Lanzone, A., Tamburrini, E., Vento, G., et al. (2020). Neonatal Late Onset Infection with Severe Acute Respiratory Syndrome Coronavirus 2. Am. J. Perinatol. *37*, 869–872.

Cantini, F., Niccoli, L., Nannini, C., Matarrese, D., Natale, M.E.D., Lotti, P., Aquilini, D., Landini, G., Cimolato, B., Pietro, M.A.D., et al. (2020). Beneficial impact of Baricitinib in COVID-19 moderate pneumonia; multicentre study. J. Infect. Published online June 24, 2020. https://doi.org/10.1016/j.jinf.2020.06.052.

Costa, S., Posteraro, B., Marchetti, S., Tamburrini, E., Carducci, B., Lanzone, A., Valentini, P., Buonsenso, D., Sanguinetti, M., Vento, G., and Cattani, P. (2020). Excretion of SARS-CoV-2 in human breast milk. Clin. Microbiol. Infect. Published online June 2, 2020. https://doi.org/10.1016/j.cmi.2020.05.027.

Cui, Y., Hosui, A., Sun, R., Shen, K., Gavrilova, O., Chen, W., Cam, M.C., Gao, B., Robinson, G.W., and Hennighausen, L. (2007). Loss of signal transducer and activator of transcription 5 leads to hepatosteatosis and impaired liver regeneration. Hepatology *46*, 504–513.

Dobin, A., Davis, C.A., Schlesinger, F., Drenkow, J., Zaleski, C., Jha, S., Batut, P., Chaisson, M., and Gingeras, T.R. (2013). STAR: ultrafast universal RNA-seq aligner. Bioinformatics *29*, 15–21.

Galbadage, T., Peterson, B.M., Awada, J., Buck, A.S., Ramirez, D.A., Wilson, J., and Gunasekera, R.S. (2020). Systematic Review and Meta-Analysis of Sex-Specific COVID-19 Clinical Outcomes. Front. Med. (Lausanne) *7*, 348.

Groß, R., Conzelmann, C., Müller, J.A., Stenger, S., Steinhart, K., Kirchhoff, F., and Münch, J. (2020). Detection of SARS-CoV-2 in human breastmilk. Lancet *395*, 1757–1758.

Gupta, A., Madhavan, M.V., Sehgal, K., Nair, N., Mahajan, S., Sehrawat, T.S., Bikdeli, B., Ahluwalia, N., Ausiello, J.C., Wan, E.Y., et al. (2020). Extrapulmonary manifestations of COVID-19. Nat. Med. *26*, 1017–1032.

Heinz, S., Benner, C., Spann, N., Bertolino, E., Lin, Y.C., Laslo, P., Cheng, J.X., Murre, C., Singh, H., and Glass, C.K. (2010). Simple combinations of lineage-determining transcription factors prime *cis*-regulatory elements required for macrophage and B cell identities. Mol. Cell *38*, 576–589.

Hennighausen, L., and Robinson, G.W. (2008). Interpretation of cytokine signaling through the transcription factors STAT5A and STAT5B. Genes Dev. *22*, 711–721.

Hoffmann, M., Kleine-Weber, H., Schroeder, S., Krüger, N., Herrler, T., Erichsen, S., Schiergens, T.S., Herrler, G., Wu, N.-H., Nitsche, A., et al. (2020). SARS-CoV-2 Cell Entry Depends on ACE2 and TMPRSS2 and Is Blocked by a Clinically Proven Protease Inhibitor. Cell *181*, 271–280.

Huber, W., Carey, V.J., Gentleman, R., Anders, S., Carlson, M., Carvalho, B.S., Bravo, H.C., Davis, S., Gatto, L., Girke, T., et al. (2015). Orchestrating high-throughput genomic analysis with Bioconductor. Nat. Methods *12*, 115–121.

Imai, Y., Kuba, K., Rao, S., Huan, Y., Guo, F., Guan, B., Yang, P., Sarao, R., Wada, T., Leong-Poi, H., et al. (2005). Angiotensin-converting enzyme 2 protects from severe acute lung failure. Nature *436*, 112–116.

Khalil, A., Kalafat, E., Benlioglu, C., O'Brien, P., Morris, E., Draycott, T., Thangaratinam, S., Doare, K.L., Heath, P., Ladhani, S., et al. (2020). SARS-CoV-2 infection in pregnancy: A systematic review and meta-analysis of clinical features and pregnancy outcomes. EClinicalMedicine *25*, 100446.

Kirtsman, M., Diambomba, Y., Poutanen, S.M., Malinowski, A.K., Vlachodimitropoulou, E., Parks, W.T., Erdman, L., Morris, S.K., and Shah, P.S. (2020). Probable congenital SARS-CoV-2 infection in a neonate born to a woman with active SARS-CoV-2 infection. CMAJ *192*, E647–E650.

La Rosée, F., Bremer, H.C., Gehrke, I., Kehr, A., Hochhaus, A., Birndt, S., Fellhauer, M., Henkes, M., Kumle, B., Russo, S.G., and La Rosée, P. (2020). The Janus kinase 1/2 inhibitor ruxolitinib in COVID-19 with severe systemic hyperinflammation. Leukemia *34*, 1805–1815.

Lackey, K.A., Pace, R.M., Williams, J.E., Bode, L., Donovan, S.M., Järvinen, K.M., Seppo, A.E., Raiten, D.J., Meehan, C.L., McGuire, M.A., and McGuire, M.K. (2020). SARS-CoV-2 and human milk: What is the evidence? Matern. Child Nutr. Published online May 30, 2020. https://doi.org/10.1016/mcn.13032.

Lamers, M.M., Beumer, J., van der Vaart, J., Knoops, K., Puschhof, J., Breugem, T.I., Ravelli, R.B.G., Paul van Schayck, J., Mykytyn, A.Z., Duimel, H.Q., et al. (2020). SARS-CoV-2 productively infects human gut enterocytes. Science *369*, 50–54.

Langmead, B., Trapnell, C., Pop, M., and Salzberg, S.L. (2009). Ultrafast and memory-efficient alignment of short DNA sequences to the human genome. Genome Biol. *10*, R25.

Lee, H.K., Willi, M., Shin, H.Y., Liu, C., and Hennighausen, L. (2018). Progressing super-enhancer landscape during mammary differentiation controls tissue-specific gene regulation. Nucleic Acids Res. *46*, 10796–10809.

Lee, J.J., Kopetz, S., Vilar, E., Shen, J.P., Chen, K., and Maitra, A. (2020). Relative Abundance of SARS-CoV-2 Entry Genes in the Enterocytes of the Lower Gastrointestinal Tract. Genes (Basel) *11*, 645.

Liu, X., Robinson, G.W., Wagner, K.U., Garrett, L., Wynshaw-Boris, A., and Hennighausen, L. (1997). Stat5a is mandatory for adult mammary gland development and lactogenesis. Genes Dev. *11*, 179–186.

Love, M.I., Huber, W., and Anders, S. (2014). Moderated estimation of fold change and dispersion for RNA-seq data with DESeq2. Genome Biol. *15*, 550.

Lukassen, S., Chua, R.L., Trefzer, T., Kahn, N.C., Schneider, M.A., Muley, T., Winter, H., Meister, M., Veith, C., Boots, A.W., et al. (2020). SARS-CoV-2 receptor ACE2 and TMPRSS2 are primarily expressed in bronchial transient secretory cells. EMBO J. *39*, e105114.

Metser, G., Shin, H.Y., Wang, C., Yoo, K.H., Oh, S., Villarino, A.V., O'Shea, J.J., Kang, K., and Hennighausen, L. (2016). An autoregulatory enhancer controls mammary-specific STAT5 functions. Nucleic Acids Res. *44*, 1052–1063.

Monteil, V., Kwon, H., Prado, P., Hagelkruys, A., Wimmer, R.A., Stahl, M., Leopoldi, A., Garreta, E., Hurtado Del Pozo, C., Prosper, F., et al. (2020). Inhibition of SARS-CoV-2 Infections in Engineered Human Tissues Using Clinical-Grade Soluble Human ACE2. Cell *181*, 905–913.

Qi, F., Qian, S., Zhang, S., and Zhang, Z. (2020). Single cell RNA sequencing of 13 human tissues identify cell types and receptors of human coronaviruses. Biochem. Biophys. Res. Commun. *526*, 135–140.

Reid, H.W., Buxton, D., Pow, I., and Finlayson, J. (1984). Transmission of louping-ill virus in goat milk. Vet. Rec. *114*, 163–165.

Risso, D., Ngai, J., Speed, T.P., and Dudoit, S. (2014). Normalization of RNA-seq data using factor analysis of control genes or samples. Nat. Biotechnol. *32*, 896–902.

Stanifer, M.L., Kee, C., Cortese, M., Zumaran, C.M., Triana, S., Mukenhirn, M., Kraeusslich, H.G., Alexandrov, T., Bartenschlager, R., and Boulant, S. (2020). Critical Role of Type III Interferon in Controlling SARS-CoV-2 Infection in Human Intestinal Epithelial Cells. Cell Rep. *32*, 107863.

Tam, P.C.K., Ly, K.M., Kernich, M.L., Spurrier, N., Lawrence, D., Gordon, D.L., and Tucker, E.C. (2020). Detectable severe acute respiratory syndrome coronavirus 2 (SARS-CoV-2) in human breast milk of a mildly symptomatic patient with coronavirus disease 2019 (COVID-19). Clin. Infect. Dis. Published online May 30, 2020. https://doi.org/10.1093/cid/ciaa673.

Thorvaldsdóttir, H., Robinson, J.T., and Mesirov, J.P. (2013). Integrative Genomics Viewer (IGV): high-performance genomics data visualization and exploration. Brief. Bioinform. *14*, 178–192.

Wickham, H. (2009). Ggplot2: elegant graphics for data analysis (Springer).

Willi, M., Yoo, K.H., Wang, C., Trajanoski, Z., and Hennighausen, L. (2016). Differential cytokine sensitivities of STAT5-dependent enhancers rely on Stat5 autoregulation. Nucleic Acids Res. *44*, 10277–10291.

Wu, Y., Liu, C., Dong, L., Zhang, C., Chen, Y., Liu, J., Zhang, C., Duan, C., Zhang, H., Mol, B.W., et al. (2020). Coronavirus disease 2019 among pregnant Chinese women: case series data on the safety of vaginal birth and breastfeeding. BJOG *127*, 1109–1115.

Yamaji, D., Kang, K., Robinson, G.W., and Hennighausen, L. (2013). Sequential activation of genetic programs in mouse mammary epithelium during pregnancy depends on STAT5A/B concentration. Nucleic Acids Res. *41*, 1622–1636.

Yuasa, K., and Hijikata, T. (2016). Distal regulatory element of the STAT1 gene potentially mediates positive feedback control of STAT1 expression. Genes Cells *21*, 25–40.

Zhao, Y., Zhao, Z., Wang, Y., Zhou, Y., Ma, Y., and Zuo, W. (2020). Single-cell RNA expression profiling of ACE2, the receptor of SARS-CoV-2. Am. J. Respir. Crit. Care Med. *202*, 756–759.

Ziegler, C.G.K., Allon, S.J., Nyquist, S.K., Mbano, I.M., Miao, V.N., Tzouanas, C.N., Cao, Y., Yousif, A.S., Bals, J., Hauser, B.M., et al. (2020). SARS-CoV-2 Receptor ACE2 Is an Interferon-Stimulated Gene in Human Airway Epithelial Cells and Is Detected in Specific Cell Subsets across Tissues. Cell *181*, 1016–1035.

STAR★METHODS

KEY RESOURCES TABLE

REAGENT or RESOURCE	SOURCE	IDENTIFIER
Antibodies		
Rabbit polyclonal anti-ACE2	Proteintech	Cat# 21115-1-AP; RRID: AB_10732845
Rabbit monoclonal anti-GAPDH	Cell signaling	Cat# 5174; RRID: AB_10622025
Chemicals, Peptides, and Recombinant Proteins		
SsoAdvanced Universal Probes Suplermix	Bio-rad	Cat# 172-5281
Critical Commercial Assays		
PureLink RNA Mini Kit	Invitrogen	Cat# 12183018A
SuperScript III First-Strand Synthesis SuperMix	Invitrogen	Cat# 18080-400
Deposited Data		
ChIP-seq and RNA-seq data	NCBI GEO dataset	GSE115370
ChIP-seq data	NCBI GEO dataset	GSE121438
ChIP-seq data and RNA-seq data	NCBI GEO dataset	GSE127139
ChIP-seq data	NCBI GEO dataset	GSE40930
ChIP-seq data	NCBI GEO dataset	GSE37646
RNA-seq data	NCBI GEO dataset	GSE148829
Mouse reference genome UCSC, mm10	UCSC Genome Browser	http://hgdownload.soe.ucsc.edu/downloads.html#mouse
Experimental Models: Organisms/Strains		
C57BL/6 mice	Charles River	N/A
Oligonucleotides		
mouse Ace2 probe (Mm01159006_m1)	Thermo Fisher scientific	Cat# 4351370
mouse *Stat5a* probe (Mm03053818_s1)	Thermo Fisher scientific	Cat# 4351370
mouse *Stat5b* probe (Mm00839889_m1)	Thermo Fisher scientific	Cat# 4351370
mouse *Cish* probe (Mm01230623_g1)	Thermo Fisher scientific	Cat# 4351370
mouse *Gapdh* probe	Applied Biosystems	Cat# 4352339E
Software and Algorithms		
Trimmomatic (version 0.36)	Bolger et al., 2014	http://www.usadellab.org/cms/?page=trimmomatic
Bowtie (version 1.1.2)	Langmead et al., 2009	http://bowtie-bio.sourceforge.net/manual.shtml
Picard		http://broadinstitute.github.io/picard/
Homer (version 4.8.2)	Heinz et al., 2010	http://homer.ucsd.edu/homer/
Integrative Genomics Viewer	Thorvaldsdóttir et al., 2013	http://software.broadinstitute.org/software/igv/
STAR (2.5.4a)	Dobin et al., 2013	https://anaconda.org/bioconda/star/files?version=2.5.4a
HTSeq	Anders et al., 2015	https://htseq.readthedocs.io/en/master/
R (3.6.3)		https://www.R-project.org/
Bioconductor	Huber et al., 2015	https://www.bioconductor.org/
DESeq2	Love et al., 2014	https://bioconductor.org/packages/release/bioc/html/DESeq2.html
RUVSeq	Risso et al., 2014	https://bioconductor.org/packages/release/bioc/html/RUVSeq.html

(*Continued on next page*)

Continued

REAGENT or RESOURCE	SOURCE	IDENTIFIER
dplyr		https://cran.r-project.org/web/packages/dplyr/index.html
ggplot2	Wickham, 2009	https://ggplot2.tidyverse.org/
PRISM GraphPad (8.2.0)		https://www.graphpad.com/scientific-software/prism/

RESOURCE AVAILABILITY

Lead Contact

Further information and requests for resources and reagents should be directed to and will be fulfilled by the Lead Contact Lothar Hennighausen (lotharh@nih.gov).

Materials Availability

This study did not generate new unique reagents.

Data and Code Availability

RNA-seq data shown in Figures 1B and 1D and ChIP-seq data shown in Figures 2, 3, and 4 were generated in our lab and deposited in the Gene Expression Omnibus (GEO). ChIP-seq and RNA-seq data of mouse lactating tissue were obtained from GEO: GSE115370, GSE121438 and GSE127139. ChIP-seq and RNA-seq data from lactating tissue from *Stat5* mutant mice were obtained from GEO: GSE40930 and GSE37646. RNA-seq data of human bronchial cell line (BEAS-2B) and airway basal cells from human donors treated with IFNa2, IFNγ, IL4 or IL17A were obtained from GEO: GSE148829.

EXPERIMENTAL MODEL AND SUBJECT DETAILS

Animals

All animals were housed and handled according to the Guide for the Care and Use of Laboratory Animals (8th edition) and all animal experiments were approved by the Animal Care and Use Committee (ACUC) of National Institute of Diabetes and Digestive and Kidney Diseases (NIDDK, MD) and performed under the NIDDK animal protocol K089-LGP-17. Two-month-old C57BL/6 female mice (Charles River) were bred and the mammary gland tissue was harvested at days 6, 13 and 19 of pregnancy (p6, p13 and p18), at day 1 and 10 (L1 and L10) after parturition, and after 24 hours of involution (I24). For the I24 time point, pups were separated from lactating dams at day 10 of lactation and tissue was harvested after 24 hours.

METHOD DETAILS

Chromatin immunoprecipitation sequencing (ChIP-seq) analysis

Quality filtering and alignment of the raw reads was done using Trimmomatic (Bolger et al., 2014) (version 0.36) and Bowtie (Langmead et al., 2009) (version 1.1.2), with the parameter '-m 1' to keep only uniquely mapped reads, using the reference genome mm10. Picard tools (Broad Institute. Picard, http://broadinstitute.github.io/picard/, 2016) was used to remove duplicates and subsequently, Homer (Heinz et al., 2010) (version 4.8.2) software was applied to generate bedGraph files, seperately. Integrative Genomics Viewer (Thorvaldsdóttir et al., 2013) (version 2.3.81) was used for visualization.

RNA-seq analysis

mRNA-seq read quality control was done using Trimmomatic (Bolger et al., 2014) (version 0.36) and STAR RNA-seq (Dobin et al., 2013) (version STAR 2.5.4a) using 50bp paired-end mode was used to align the reads (mm10). HTSeq (Anders et al., 2015) was to retrieve the raw counts and subsequently, R (https://www.R-project.org/), Bioconductor (Huber et al., 2015) and DESeq2 (Love et al., 2014) were used. Additionally, the RUVSeq (Risso et al., 2014) package was applied to remove confounding factors. The data were pre-filtered keeping only those genes, which have at least ten reads in total. Genes were categorized as significantly differentially expressed with an adjusted p value (pAdj) below 0.05 and a fold change > 2 for upregulated genes and a fold change of < -2 for downregulated ones. The visualization was done using dplyr (https://cran.r-project.org/web/packages/dplyr/index.html) and ggplot2 (Wickham, 2009).

Western blot

Proteins (100 μg) from mouse mammary tissues were extracted with lysis buffer (50 mM Tris-Cl pH 8.0, 150 mM NaCl, 0.5% Na-DOC, 1% NP-40, 0.1% SDS, 5 mM EDTA, 1 mM PMSF, and protease inhibitor cocktail), separated on a 4%–12% NuPage gradient gel

(Invitrogen) and transferred to a PVDF membrane (Invitrogen). Membranes were blocked for 1 h with 5% nonfat dry milk in PBS-T buffer (PBS containing 0.1% Tween 20) and incubated for 1.5 hr at 4°C with the primary antibody against ACE2 (Proteintech, 21115-1-AP) and GAPDH (Cell signaling, #5174). After washing, membranes were incubated for 1 h with HRP-conjugated secondary antibodies (Cell signaling). Labeled protein bands were detected using an enhanced chemiluminescence system (Thermo scientific) and Amersham Imager 600 (GE healthcare). Band density was analyzed using this imager.

RNA isolation and quantitative real-time PCR (qRT–PCR)

Mammary tissues were harvested from non-parous and day 10 of lactating female mice and homogenized using an electronic homogenizer. RNA was extracted using the PureLink RNA Mini Kit (Invitrogen) according to the manufacturer's instructions. cDNA was synthesized from total RNA using Superscript II (Invitrogen). Quantitative real-time PCR (qRT-PCR) was performed using TaqMan probes (Ace2, Mm01159006; *Stat5a*, Mm03053818; *Stat5b*, Mm00839889; *Cish*, Mm01230623, Thermo Fisher scientific; mouse *Gapdh*, 4352339E, Applied Biosystems) on the CFX384 Real-Time PCR Detection System (Bio-Rad) according to the manufacturer's instructions. PCR conditions were 95°C for 30 s, 95°C for 15 s, and 60°C for 30 s for 40 cycles. All reactions were done in triplicate and normalized to the housekeeping gene *Gapdh*. Relative differences in PCR results were calculated using the comparative cycle threshold (C_T) method.

QUANTIFICATION AND STATISTICAL ANALYSIS

For comparison of samples, data were presented as standard deviation in each group and were evaluated with a t test and ANOVA multiple comparisons using PRISM GraphPad. Statistical significance was obtained by comparing the measures from wild-type or control group, and each mutant group. A value of $^{*}p < 0.05$, $^{**}p < 0.001$, $^{***}p < 0.0001$, $^{****}p < 0.00001$ was considered statistically significant.